JOURNAL OF AIRCRAFT
Vol. 33, No. 1, January–February 1996

Helicopter Flight Data Feature Extraction or Component Load Monitoring

David J. Haas,* Lance Flitter,† and Joel Milano‡
U.S. Naval Surface Warfare Center, Bethesda, Maryland 20084-5000

Helicopter flight data are analyzed using univariate and multivariate techniques to extract features of relevance for rotor system component load prediction. The vibratory component of four rotor system loads is examined; main rotor pushrod, rotor blade normal bending, lag damper, and main rotor shaft bending load. Univariate relationships between these loads and fixed system parameters are examined and basic trends are highlighted. Multivariate approaches including multiple linear regression and artificial neural network analyses are utilized to create load prediction models. Fixed system parameters form the basis of the models and include pilot control positions and aircraft state parameters. Generally, the loads can be predicted quite well during steady level flight, as well as moderate and high-*g* flight where fatigue damage is most likely to occur. Low speed and hovering flight and flight conditions with low engine torque are the most difficult flight conditions for accurate load prediction. Significant parameters in the regression and neural network models are identified and several flight regimes are defined that can be used to improve load prediction accuracy.

Introduction

AN increasing emphasis has been placed on health and usage monitoring systems for helicopters in an effort to improve reliability and significantly reduce operating costs. The focus of these systems has been directed towards engine and drive-train monitoring as well as individual aircraft usage monitoring.[1,2] Aircraft usage monitoring provides the benefit of utilizing actual aircraft usage data rather than relying on an assumed mission usage spectrum. If actual usage between aircraft varies significantly, fatigue life assessments based on an assumed spectrum may contain a high degree of conservatism. This is because the assumed spectrum must include the worst-case scenario. Individual aircraft usage monitoring eliminates this aspect of conservatism in rotor component fatigue life assessment while maintaining safety requirements.

Another area in fatigue life assessment that requires a high degree of conservatism is the assumed load level assigned to each maneuver in the aircraft's usage spectrum. Typically, a flight loads survey is performed to measure loads in critical, fatigue-limited rotor components to determine the worst-case load encountered for each maneuver type. This load is applied for the duration of the maneuver to calculate the fatigue life expended. If a load monitoring system could monitor the actual flight loads during a maneuver, the high degree of conservatism in this aspect of fatigue life assessment could also be eliminated.

Researchers have been investigating practical techniques to predict and monitor rotor system component loads. To avoid the complexity of slip rings and instrumentation in the rotating system, these efforts have focused around using fixed system parameters as the basis for predicting loads in the rotating system. In Refs. 3 and 4 a holometric approach is used to select strain gauge data and load measurements in the helicopter fixed system to predict rotor system component loads. These studies focused on the AH-64 helicopter. In Refs. 5 and 6, the present authors developed load prediction models for SH-60 helicopter rotor system components using only aircraft state parameters such as velocity, rate-of-climb, aircraft accelerations, and aircraft control inputs. This approach reduces the need for additional strain gauges or load measurements in the fixed system and relies on parameters that may typically be measured in an onboard aircraft flight data recorder system.

The objective of the present study is to analyze a flight loads data set that includes a broad range of flight maneuvers and identify features with relevance to helicopter load monitoring. The approach is to apply several multivariate techniques to the data and identify important features such as fixed system parameters most useful for component load prediction, differences between various component loads, significant flight regimes, and the effect of calibration data set selection on load prediction accuracy.

Flight Test Data

The flight data analyzed in this study consist of several rotor system component loads for an SH-60 helicopter measured during flight tests of many different maneuvers contained in the SH-60 usage spectrum. Over 150 distinct maneuvers are analyzed. The duration of each flight maneuver varies from approximately 10 to 60 s. The data consist of over 18,000 individual data points each representing a particular instant in time and corresponds to approximately 40 min of flight time. Hovering flight as well as high-speed and high-*g* flight is represented.

Four rotor system loads are studied that represent flap, lag, torsion, and shaft bending loads. The four component loads selected consist of pushrod, blade normal bending, lag damper, and main rotor shaft bending load. It is felt that these loads exhibit behavior that is indicative of overall rotor system behavior. The focus of this study is on analysis and prediction of the vibratory component of load since it is most directly related to fatigue life expended on a given component. Table 1 shows the list of 18 independent parameters that are used for the prediction of rotor system component loads. In this study, the flight maneuvers are divided into 10 different

Presented as Paper 94-1308 at the AIAA 35th Structures, Structural Dynamics, and Materials Conference, Hilton Head, SC, April 18–21, 1994; received June 11, 1994; revision received June 23, 1995; accepted for publication July 5, 1995.

*Aerospace Engineer, Sea Based Aviation Office, David Taylor Model Basin Carderock Division. Senior Member AIAA.

†Computer Scientist, Systems Directorate, David Taylor Model Basin Carderock Division, Member AIAA.

‡Electrical Engineer, Systems Directorate, David Taylor Model Basin Carderock Division. Member AIAA.

Table 1 Predictor variables

Parameter	Abbreviation
Accelerations	
Load factor	LF
Longitudinal	$\ddot{x}$
Lateral	$\ddot{y}$
Pitch	q
Roll	p
Yaw	r
Velocity	V
Aircraft mass	m
Rate-of-climb	ROC
Altitude	h
Engine torques	Q_1, Q_2
Rotor rotation rate	Ω
Pilot control positions	
Collective	θ_0
Longitudinal cyclic	θ_{1s}
Lateral cyclic	θ_{1c}
Pedal	θ_t
Stabilator position	θ_{stab}

Table 2 Maneuver groups

Hover (approach, jump takeoff, control reversals, turns)
Level flight (20–100%V_{max})
Turns (left/right turns at various airspeeds and bank angles)
Climbs (at various airspeeds, left/right climbing turns)
Dives (at various airspeeds)
Partial power descent
Sideslips
Control reversals
Pulls (symmetric/rolling pullouts, pushovers)
Autos (autorotation, autorotative pullouts and control reversals)

maneuver groups as shown in Table 2. Each maneuver group contains a subset of specific maneuvers. For example, the hover maneuver group consists of approach to hover, hover control reversals, jump takeoff, and hover in and out of ground effect.

Approach

The technical approach is divided into two categories: 1) data-oriented and 2) model-oriented analysis. Data-oriented analysis consists of various statistical and graphical analyses of the data to make inferences directly from the data. This is in contrast to model-oriented analysis where various load prediction models are developed using multiple regression and artificial neural networks. The models are tested and used to make inferences about the component load data. The approach can be summarized in four steps: 1) analyze raw data and select data subsets, 2) define a model structure, 3) select model inputs and calibrate model using known I/O pairs, and 4) validate results, make improvements, and repeat process if necessary.

Data-Oriented Analysis

The data-oriented analysis consists primarily of calculating several descriptive statistics and analyzing various plots of the data. The purpose of these analyses are threefold: 1) to discover important features of the data, 2) to aid in defining appropriate subsets of the data for calibration and validation of predictive models, and 3) to better understand results garnered from the load prediction models.

Calculating statistics for different types of flight maneuvers provides an indication of what types of maneuvers produce damaging load levels in various rotor components. Scatter plots of component loads vs independent variables provide a graphical method to identify univariate trends in the data. Scatter plots also provide information that is useful in creating derived parameters to increase the correlation between predictor variables and loads.

A critical step in developing a load prediction model, regardless of the model approach, is the selection of a calibration data set. The calibration data set is used to calculate the regression coefficients and for training the neural network models to determine the connection weights. A properly chosen calibration data set will be an unbiased sample of the flight conditions that the model is expected to predict. The calibration data is selected using engineering judgment to select data from an equal distribution of maneuvers contained in Table 2. To confirm that the calibration data set is representative of all the data analyzed, a second randomly selected data set with the same number of data points is used for comparison.

Model-Oriented Analysis

In the model-oriented analysis, load prediction models are developed using both multiple regression and artificial neural networks (ANN). These models are used to examine the significance of various features and data subsets. Multiple regression has the advantage of producing an explicit equation that is straightforward to interpret. The relative importance of various parameters can be easily assessed. The primary disadvantage of multiple regression is that nonlinearities in the solution space can be difficult to include without extensive a priori knowledge. An advantage of ANNs is that once a particular paradigm is chosen, no a priori knowledge of the problem is required. Neural networks are also inherently nonlinear because of the nonlinear activation function contained in each processing element and can capture nonlinear characteristics of the solution space. Unfortunately, neural network models are much more difficult to interpret than a regression equation because the information is stored in an abstract form. Comparisons between these two types of models provide some indication of the degree of nonlinearity inherent in the solution space. A brief description of each modeling technique is given next.

The multiple linear regression model is expressed as

$$Y(t) = a_1X_1(t) + a_2X_2(t) + \cdots a_nX_n(t) + \text{error}$$

where X_i are the independent predictor variables, $Y(t)$ is the component load, and the a_i are the unknown regression coefficients that are solved for using a least-squares method. One advantage of a regression approach is that the exact nature of the model is known and the relative importance of the X_i can be determined for a given model. The absolute importance of a variable can never be fully determined due to model misspecification resulting in an error term. The relative importance of a given X_i is determined by standardizing the regression coefficients.

In this study, the X_i are selected using a stepwise selection process. Although the regression equation structure must be specified, the stepwise selection procedure provides a means to add and remove predictor variables to the regression equation based on their improvement to the model, their significance level, and the degree of similarity and dependence with other variables in the equation. Thus, the stepwise method provides a powerful approach to efficiently analyze many different combinations of parameters in the regression equation and helps to prevent overspecification of the model. Although the regression equation is linear, nonlinearities can be introduced by using nonlinear derived parameters for the X_i rather than the basic form of the predictor variables.

A typical neural network architecture (Fig. 1) consists of an input layer, one or more hidden layers, and an output layer. Each layer contains one or more nodes. For the load models developed in this study the input consists of the 18 predictor variables and the output consists of the predicted load. The hidden layers contain many simple processing ele-

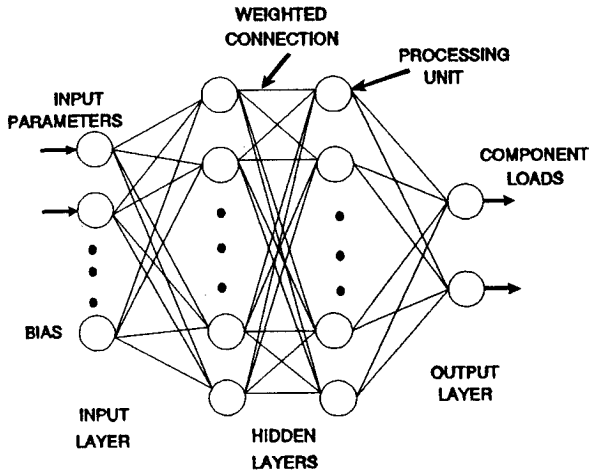

Fig. 1 Structure of a typical neural network.

ments referred to as nodes that contain a summing function and a nonlinear activation function. A typical activation function is the sigmoidal function because it is a nonlinear function that compresses the activation level to a consistent range. The nodes in each layer are interconnected by a series of weighted connections. Data flows through the network from the input to the output. In this study, the neural network is trained using supervised learning. In this approach, the neural network is exposed to a set of known I/O pairs and the connection weights are iteratively adjusted to minimize the rms error in the output. The network architecture and learning rate are taken from Ref. 6 and consist of a single hidden layer model with five nodes and a single output.

Neural networks provide a general nonlinear approach for determining the relationship between the predictor variables and the component load. One drawback of the neural network approach is that it is difficult to determine the nature of the relationship between input and output resulting in a black box type of model.

Three measures-of-fit are used to assess the results of the regression and ANN models for the calibration and validation data sets. The Pearson's correlation coefficient R is a measure of the linear relationship between two variables. A strong linear relationship results in a correlation near 100%. If no linear relationship exists the correlation will be 0%. The correlation between actual and predicted load provides an overall indication of the linear relationship between these values across the entire load range.

The second parameter used to quantify the results in the rms error for the data set. To make the rms error more comparable between loads it is normalized by the maximum value of the load in either the calibration or validation data set. A third approach used to assess the model results in a scatter plot of predicted load vs actual load. This type of plot provides a visual indication of how well the model predicts the data. A perfect model would result in all of the data falling on the 45-deg line on the plot. Scatter plots are most effective for analyzing outliers where the predicted value is far from the actual value.

Results and Discussion

Univariate Trends

The first step in analyzing features within the data is to look for univariate trends. Figures 2a and 2b show pushrod and blade bending loads vs aircraft velocity. Aircraft velocity is normalized by V_{max}, the maximum level flight velocity. All of the data points are included on the plot and represent all 10 maneuver groups as well as various aircraft weights and altitudes. The plots illustrate the necessity of utilizing multivariate techniques that can account for interactions between

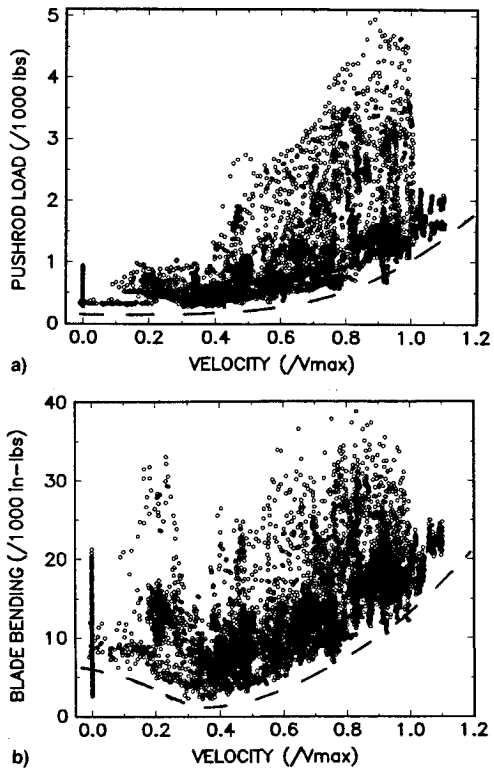

Fig. 2 Component load vs velocity: a) pushrod and b) blade bending loads.

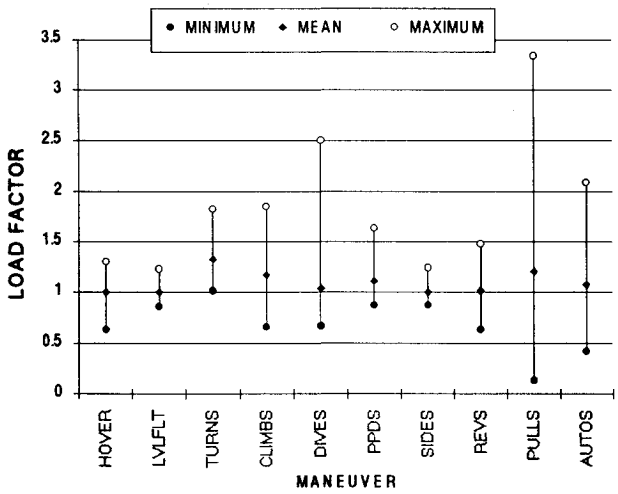

Fig. 3 Load factor range for various maneuvers.

variables to predict component loads. However, some overall trends can be established from the univariate plots. For example, Fig. 2a shows a general trend (indicated by the dashed line) of increasing pushrod load with velocity. Also, it shows that the load range varies significantly at high airspeed, whereas, at low velocity the pushrod load always remains fairly low.

A different trend is seen for blade normal bending load, (Fig. 2b). Blade bending possesses an even stronger trend of increasing load with increasing velocity than pushrod load, but the load range at a fixed velocity is more uniform across the entire velocity range. Even at low speeds a significant load level is possible. The overall trend of blade bending load with velocity (dashed line) looks similar to a typical helicopter power-required curve. High values are present in hover and decrease to a minimum near V equal to 0.35 (approximately 60 kn). Above this speed bending load increases rapidly with velocity. Damper and shaft bending loads contain a less obvious pattern with velocity.

Another way of visualizing overall trends in the data is to analyze the variability that exists in a particular parameter and how it varies for different types of maneuvers. Figure 3 is a plot of the minimum, maximum, and mean values of load factor for the 10 maneuver groups contained in Table 2. It shows that hover, level flight, side slips, and control reversals all have load factors less than 1.5 g, whereas turns, climbs, dives, partial power descents, pullouts, and autorotative maneuvers exhibit a much larger range. The larger range of load factor indicates that the rotor is transmitting high loads to the aircraft during these types of maneuvers.

Figure 4 shows a plot of pushrod and damper load vs load factor. The correlation is 52 and 37%, respectively. Figure 4a shows an overall trend of increasing pushrod load with load factor. It appears from Fig. 4b that a nonlinear relationship exists between damper load and load factor. One way to account for nonlinearities in the data is to develop derived parameters. These parameters are derived from the 18 basic parameters in Table 1 by combining and modifying them into a new nonlinear form. One notable parameter $LFm\mu$, taken from Ref. 5, is defined as the product of load factor, aircraft mass, and rotor advance ratio. The advance ratio μ is defined as the aircraft velocity divided by rotor tip speed. The variation of pushrod and damper load with this derived parameter is illustrated in Fig. 5 and results in an increase in the univariate correlation from 52 to 84% for pushrod. A strong linear relationship can be seen in the plot, especially for moderate and low loads. The overall correlation for damper load increases from 37 to 73%, but a strong nonlinear relationship is still evident. However, a fairly linear relationship exists for moderate to large values of the quantity $LFm\mu$. A list of derived parameters used in this study is given in Table 3.

Data Set Selection

To develop a regression or neural network load prediction model a calibration data set must be selected. This data is used to solve for the regression coefficients and for training the neural network. Also, a separate validation data set is selected to assess the accuracy of the models. The calibration and validation data sets should be accurate and unbiased samples of the population they represent. A larger validation data set is desirable to provide confidence in model evaluations.

The calibration data is selected using engineering judgment to select an even distribution of various flight conditions and flight maneuvers. Ideally the calibration data should be selected to avoid biasing towards one particular maneuver or flight condition. The data should encompass the full range of operating limits so that the models are interpolating rather than extrapolating. To accomplish this, 3–5 distinct flights

Table 3 Derived parameters

Parameter	Definition
Controls	θ_0, θ_{1s}, δ_{1c}, δ_t, θ_{stab}
Accelerations	$\lvert q\rvert$, $\lvert p\rvert$, $\lvert r\rvert$, $\lvert qp\rvert$, $\lvert qr\rvert$, $LF\ddot{x}$, $(LF-1)m$, $(LF-1)^2m$
Force terms	$\lvert\ddot{x}\rvert m$, $\lvert\ddot{y}\rvert m$, $LFm\mu$
Control couples	(θ_0, θ_{1s}), $(\theta_0\delta_{1c})$, $(\theta_0\delta_t)$, $(\theta_{1s}\delta_{1c})$
Velocity couples	$(\theta_0 V)$, $(\theta_{1s}V)$, $(\delta_{1c}V)$, $(\delta_t V)$
Miscellaneous terms	Q_t, h, V, ROC, m, μ, Ω, V^2, V^3, V/m, Vm, V_t

$Q_t = Q_1 + Q_2$, $V_t = (V^2 + ROC^2)^{1/2}$ and δ_{1c} and δ_t represent perturbations in θ_{1c} and θ_t from the trim setting.

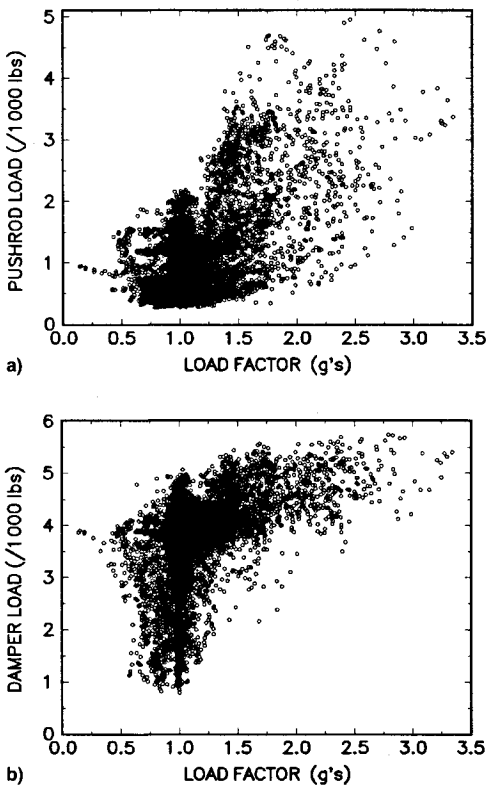

Fig. 4 Component load vs load factor: a) pushrod and b) damper loads.

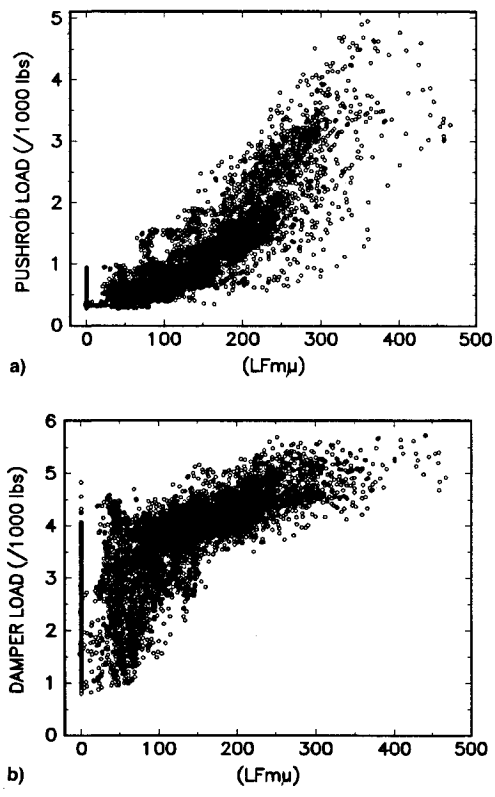

Fig. 5 Component load vs derived parameter $LFm\mu$: a) pushrod and b) damper loads.

from each of the 10 maneuver groups are chosen that represent the endpoints for the limiting features of each maneuver. For example, a left and right climb at high and low velocity are selected for the climb maneuver group. Typically a high-g and low-g variation of each maneuver is selected. Since many of the maneuvers contain a significant portion of level flight just prior to and after the maneuver, only two level flight maneuvers are selected for the calibration data set so as not to bias the calibration data towards the level flight condition. A total of 43 distinct maneuvers are selected for the calibration data that contains over 5400 data points and represents approximately 10 min of flight time.

The validation data set is also selected to represent the 10 maneuver groups. It contains nominally 10 distinct flights from each of the maneuver groups listed in Table 2. The flights within each group are selected to represent the full range of variability for that maneuver (not just the endpoints). For example, for the turn maneuver group, both left and right turns at 15-, 30-, and 45-deg angle of bank and at several airspeeds are selected. For level flight, 20 distinct flights are selected to represent the entire airspeed range from $0.2V_{max}$ to V_{max} and at several gross weights. In total, the validation data include 111 distinct flight maneuvers with over 12,500 data points and represent approximately 30 min of flight.

Flight Regime Definitions

To determine where the models perform well and where improvements are needed, the data is segmented into different categories. One obvious method to categorize the data is by maneuver type and this approach was initially tried. The maneuver descriptions provide a good overall indication of what type of conditions exists during a given maneuver, however, many maneuvers involve a range of flight conditions from mild to severe. For example, a pullout may contain data corresponding to steady level flight, descending flight, as well as moderate- and high-g conditions. For most aggressive maneuvers, the actual time spent in a high load condition is usually only a fraction of the total maneuver flight time. For this reason the data set is segmented into five different flight regimes. Each data point is uniquely assigned a flight regime based on the value of certain parameters such as load factor, velocity, engine torque, etc. Five flight regimes are defined for the purposes of this study and are given in Table 4. Most of the data fall into regime 3, moderate-g flight. This is ex-

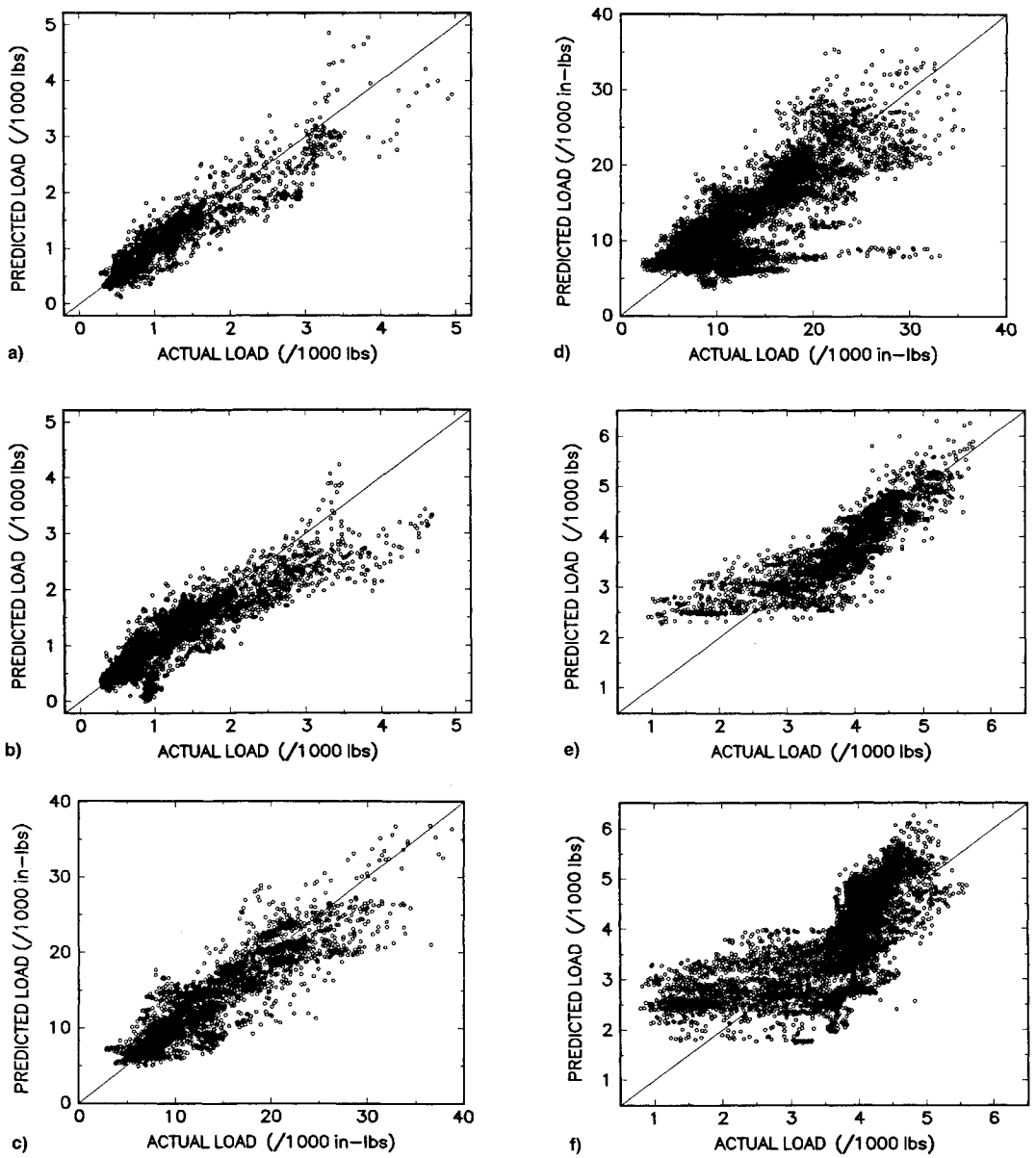

Fig. 6 Baseline regression results: a) pushrod load, calibration data; b) pushrod load, validation data; c) blade bending, calibration data; d) blade bending, validation data; e) damper load, calibration data; and f) damper load, validation data.

Table 4 Flight regime definitions

Regime no. and description	Definition
1. Hover/low-speed	$V < 0.4$, $Q_t \geq 50\%$
2. Steady level flight	$V \geq 0.4$, $Q_t \geq 50\%$
	$0.9\ g \leq LF \leq 1.1\ g$
	$\lvert ROC \rvert \leq 200$ fpm
	$\lvert \ddot{x} \rvert \leq 0.075\ g$
	$\lvert \ddot{y} \rvert \leq 0.05\ g$
	$\lvert p \rvert, \lvert r \rvert, \lvert q \rvert \leq 7.5$ deg/s^2
3. Moderate g	$LF < 1.5\ g$
	$V \geq 0.4$, $Q_t \geq 50\%$[a]
4. High g	$LF \geq 1.5\ g$
	$V \geq 0.4$, $Q_t \geq 50\%$
5. Partial power	$Q_t < 50\%$

[a]Not contained in regime no. 2.

Table 5 Model prediction results

	Regression models	
Load	CDS	VDS
Pushrod	94–4.2	91–5.6
Blade bending	91–6.3	81–9.4
Damper	87–6.8	72–11.3
Shaft bending	88–5.3	57–10.3
	Neural network models	
	CDS	VDS
Pushrod	97–2.8	93–4.8
Blade bending	96–4.4	85–8.4
Damper	94–4.9	77–10.0
Shaft bending	95–3.6	77–7.8

CDS, calibration data; VDS, validation data; R–rms error, in %.

pected since the data represent a broad range of maneuvers and the extreme flight conditions occur only for a limited time.

Baseline Regression Models

Regression models for each of the four loads are developed based on the calibration data using the derived parameters in Table 3. The resulting equations contain from 12 to 16 terms. Scatter plots of predicted vs actual load for the pushrod, blade bending, and damper models are shown in Figs. 6a–6f for both calibration and validation data sets. The correlation and normalized rms error are summarized for all four loads in Table 5. The rms error is normalized by the maximum load in the data set being evaluated and is expressed in percent. Correlations above 90% are attained for the calibration data for both pushrod and normal bending loads. The correlations for pushrod on the validation data is 91% with a 5.6% rms error and the prediction is generally very good except at high loads. This is most likely due to the low load bias in the calibration data set that is evident in Fig. 6a by the heavy concentration of data in the low load range.

Prediction of blade normal bending load in the validation data results in an 81% correlation with a 9.4% rms error. The blade bending load model has greater scatter than the pushrod load, but the data points are more evenly distributed about the ideal 45-deg line. It is obvious in Fig. 6d that one maneuver is severely underpredicted as indicated by the horizontal string of data points corresponding to a predicted load of about 7500 in.-lb. These data points correspond to an approach to hover where the aircraft is descending and slowing. This maneuver is not directly represented in the calibration data, but did not stand out for the other three loads.

Results for damper load (Figs. 6e and 6f), show a distinctly different trend. Although a correlation of 87% is attained for the calibration data the low load range is severely overpredicted. This nonlinear trend is even more dramatic in the validation data where the correlation is 72% and the normalized rms error is 11.3%. From Fig. 6f it is seen that below a load of 3500 lb the model predicts a horizontal trend with a large degree of scatter. Above 3500 lb, model accuracy significantly improves, but the load is still somewhat overpredicted.

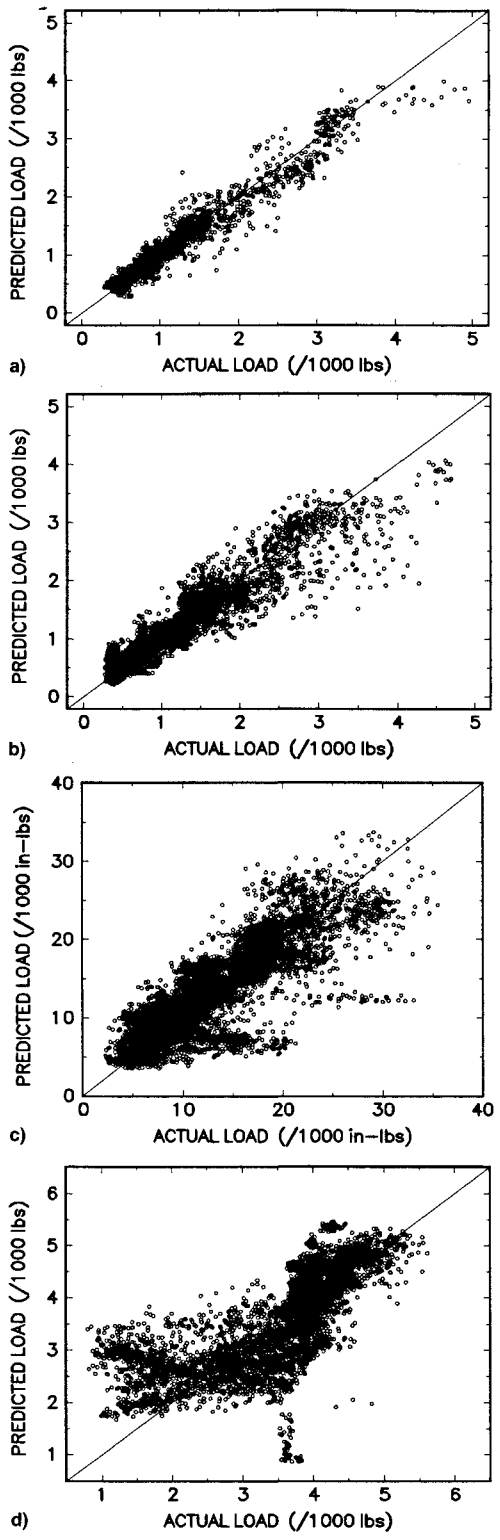

Fig. 7 Baseline neural network results: a) pushrod load, calibration data; b) pushrod load, validation data; c) blade bending, validation data; and d) damper load, validation data.

The shaft bending data (not shown) are primarily concentrated near the lower end of the load range with only a relatively few data points at a high load level. This results in a relatively low correlation of 57% (compared to the other loads) and a normalized rms error of 10.3%.

Baseline Neural Network Models

A neural network model for each load was also developed. The scatter plots of predicted vs actual load for the pushrod model are shown in Figs. 7a and 7b for both the calibration and validation data. Figures 7c and 7d show the validation results for the blade bending and damper models. The correlations and rms error are summarized in Table 5 for all of the neural network models. The results are quite similar to the regression model results. Overall, the neural network performs slightly better with rms errors approximately 10% lower than the regression models. From Fig. 7b it is seen that the neural network predicts low pushrod loads very well, but underpredicts the high load data similar to the regression model. Neural network results for blade normal bending load (Fig. 7c) are also quite similar to the regression results.

For the damper load the neural network trains very well, but exhibits the same nonlinearity in the validation data (Fig. 7d) that was present in the regression model. The network predicts damper loads above 4000 lb quite well, but exhibits a high degree of scatter and overprediction for loads below this. A set of outliers is seen in Fig. 7d where the actual load is about 3600 lb. These data points correspond to a run-on landing maneuver at 20 kn, which is not represented in the calibration data. The shaft bending load improved significantly over the regression model results with correlation increasing from 57 to 77% and an rms error reduction of 25%. The general increase in accuracy of the neural network as compared to the regression equations is probably due to the neural network's ability to represent nonlinearities implicitly.

For comparison purposes, regression and neural network models were developed using a calibration data set randomly selected from the data analyzed. The resulting scatter plots appear nearly identical to those presented in Figs. 6 and 7. This suggests that the calibration data selected by engineering judgment is representative of the population.

Model Evaluations and Improvements

Results for the regression and neural network models presented in Figs. 6 and 7 provide limited information regarding where the models perform well and where they need improvement. To examine strengths and weakness in the load models the prediction accuracy is analyzed separately for each flight regime. The validation data is separated into five flight regimes and the correlation and rms error for the baseline neural network and regression models are calculated for each regime. Validation results are summarized in Table 6. For pushrod load both regression and neural network models show that the high-g flight regime has the largest rms error. This regime represents the high load data points that are underpredicted in Figs. 6b and 7b. The other four regimes are predicted quite well for pushrod load as is reflected by the much lower rms error. For blade normal bending, damper, and shaft bending loads the highest rms error is found in the hover and low-speed flight regime making this flight regime the most difficult for prediction of these loads.

To improve prediction accuracy in regimes with high rms error, regime-specific models were developed for each flight regime. The correlation and rms error for these models are summarized in Table 7. For the regression model the results for regime 4, high-g maneuvers are significantly improved compared to the baseline results (Table 6) for all of the loads except blade bending. Pushrod models for both regimes 3 and 4 are significantly improved.

Utilizing the baseline pushrod model for regimes 1, 2, and 5 and the regime-specific model for regimes 3 and 4 produces

Table 6 Baseline regression and neural network results for regimes

	Regression models, regime				
Load	1	2	3	4	5
Pushrod	44–3.0	93–2.8	91–5.3	91–13.3	83–6.4
Blade bending	14–12.2	89–6.6	88–7.7	79–11.9	61–11.4
Damper	59–14.4	68–8.5	72–9.8	56–10.0	62–13.3
Shaft bending	42–11.7	3–11.1	44–9.2	72–14.6	82–9.9
	Neural network models, regime				
	1	2	3	4	5
Pushrod	30–4.5	91–3.7	94–4.4	89–11.2	90–4.2
Blade bending	31–12.2	93–5.4	91–6.5	78–12.0	66–9.2
Damper	59–15.6	54–5.5	79–7.4	66–6.2	70–12.4
Shaft bending	43–10.7	89–4.5	75–5.9	77–13.0	83–9.4

R–rms error for validation data set, in %.

Table 7 Regime-specific regression and neural network results

	Regression models, regime				
Load	1	2	3	4	5
Pushrod	56–3.0	63–9.4	93–4.6	94–7.7	82–7.0
Blade bending	15–13.4	92–6.7	91–6.7	74–12.7	59–12.4
Damper	60–14.2	35–25.3	76–6.8	71–5.6	63–17.9
Shaft bending	39–12.6	24–12.4	48–8.4	90–9.1	67–15.4
	Neural network models, regime				
	1	2	3	4	5
Pushrod	43–3.9	96–2.3	93–4.7	91–9.8	86–5.6
Blade bending	38–12.4	91–8.2	91–6.7	72–13.5	72–8.5
Damper	29–23.0	62–6.8	82–6.1	62–6.6	70–13.5
Shaft bending	10–20.2	34–9.9	46–8.8	77–14.4	62–17.0

R–rms error for validation data set, in %.

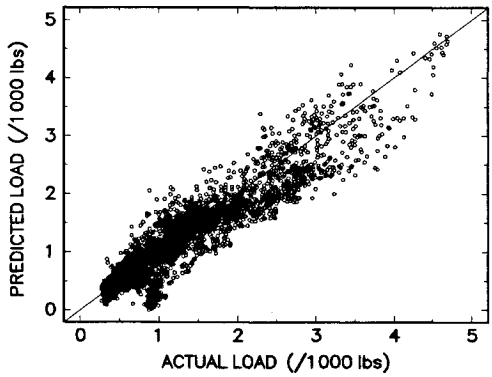

Fig. 8 Regime-specific regression model for pushrod load.

an overall regression model for pushrod load with high accuracy in all five flight regimes. The scatter plot for the validation data is shown in Fig. 8. The overall correlation for the validation data is 93% and the rms error is 4.8%. The regime-specific neural network model for pushrod also showed improvement for regimes 1, 2, and 4. However, regime 4 was still the most difficult regime for the neural network model to predict.

Analysis of shaft bending in regime 4 shows significant improvement when using a regression model specialized for this flight regime. The correlation increased from 72 to 90% and the rms error reduced by more than one-third. The shaft bending model for regime 3 also produced lower rms error (Table 7). The regime-specific neural network model did not improve results for shaft bending load for any of the flight regimes.

The regime-specific models for damper load using regression or neural networks revealed that relatively good models exist for regimes 2, 3, and 4, whereas even using regime-specific models for regimes 1 and 5 does not improve the accuracy in these two regimes. Using regime-specific models for blade bending load did not improve the overall ability to predict this load and an alternative approach is needed for further improvement in predicting this load. The regime-specific models help to illustrate under what flight conditions a satisfactory prediction model can be developed for a given load. Also, they highlight where alternative modeling approaches are needed.

It is evident that both the regression and neural network damper models are inappropriate and unable to accurately predict damper load over the complete load range. The most likely explanation for this is that the lag damper is distinctly different from the other three components. The main rotor pushrod, blade spar, and shaft are all metallic components with constant stiffness properties and they deform in a linear manner with an applied force. Conversely, the damper is a hydraulic system whose response characteristics vary significantly for different flight conditions and in a nonlinear manner. At the rotor rotation frequency, the damper force is a nonlinear function of the damper stroke velocity that is related to rotor blade lag motion. At low stroke velocities, the damper force increases rapidly with increasing stroke velocity. As the damper force increases to approximately 3500 lb, pressure relief valves in the damper open to limit the damper force. Thus, damper characteristics are highly dependent on the load level. For loads below approximately 3500 lb the characteristics are nonlinear and vary significantly with damper stroke velocity. For loads above approximately 3500 lb the damper characteristics become more constant.

Because of the unique nonlinear nature of damper load several alternative approaches are examined to predict this load. The first approach is a maneuver-specific approach where a separate neural network is trained for each of the 10 flight maneuvers contained in Table 2. The neural networks trained very well with a correlation of 96% and a normalized rms error of 3.9%. However, applying the model to the validation data shows that a high degree of uncertainty in predicted damper load exists below 4000 lb (Fig. 9). Above 4000 lb the model works very well.

To further investigate the effect of load level on damper load prediction, a neural network model is segmented by load level. One network is trained using loads below 3800 lb and one is trained for loads above 3800 lb. Again, the network trained very well for all load levels, but only accurately predicted validation data loads above 3800 lb. The results appear very similar to Fig. 9. Similarly, a regression model based on loads above and below 3800 lb is developed. These two models are applied to the entire validation data separately to examine how well they predict loads across the entire load range. The regression equation based on low load data does poorly for the entire validation data, whereas, the regression model based on high load data predicts high loads in the validation data very well (Fig. 10). The rms error for this model for loads above 3800 lb is only 5.3%. As with all of the previous damper models, the high-load regression model for damper also overpredicts the low damper loads, although with a fairly low level of scatter.

These results show that a prediction model for the damper that reliably predicts loads above approximately 3800 lb for all of the maneuvers and flight regimes is possible. Generally, damper loads in this range occur in regimes 2, 3, and 4. This high-load damper model also provides a reliable upper bound prediction of damper loads below 3800 lb in all flight maneuvers and regimes examined in this study and can therefore be used without a priori knowledge of the load level or flight condition. Because the endurance limit corresponding to the damper load is above 4000 lb, this model could be utilized to predict fatigue damaging loads. However, an alternative modeling approach is necessary to accurately predict damper loads below 3800 lb.

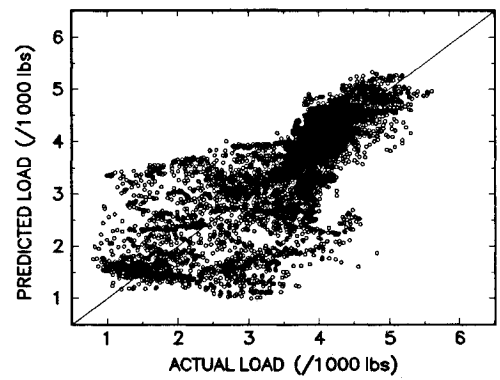

Fig. 9 Maneuver-specific neural network model for damper load.

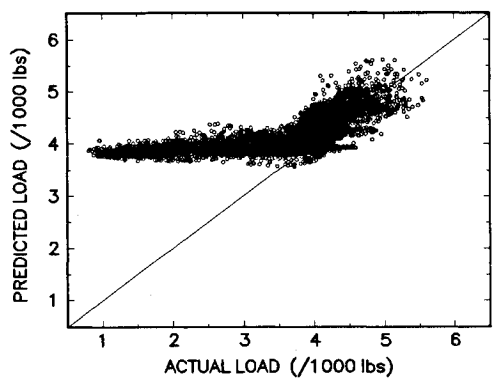

Fig. 10 Regression model segmented by load level for damper load (validation data using high-load model).

Table 8 Significant parameters in load models

Regression models			
Pushrod	Blade bending	Damper	Shaft bending
$LFm\mu$	$LFm\mu$	$LFm\mu$	$(\theta_{1s}V)$
$(\theta_{1s}V)$	$(\theta_{1s}V)$	Q_t	$\lvert\ddot{x}\rvert m$
V/m	V/m	h	$\lvert pr\rvert$
$(LF-1)^2m$	$(\theta_{1s}\delta_{1c})$	$\lvert\ddot{x}\rvert m$	θ_{stab}
			m
			$(\theta_{1s}\delta_{1c})$
			$(\theta_0\delta_{1c})$
Neural network models			
LF	V	V	LF
V	LF	LF	Q_2
Q_1	θ_{1s}	Q_1	V
θ_{1s}	Q_1	h	$\ddot{x}$
		θ_{1s}	m
			θ_{1s}

Evaluation of Significant Parameters

The most significant parameters in the regression equations, as determined from the standardized regression coefficients, for the four loads are presented in Table 8. The important parameters include combinations of load factor, velocity, pilot longitudinal stick position, and aircraft mass. Pushrod and blade bending loads have almost identical makeup and the derived parameter consisting of the quantity $LFm\mu$ is a major term in the equations for pushrod, blade bending, and damper loads. The shaft bending load has a somewhat different set of terms than the other loads.

Examining the significant parameters in the neural network models is not as straightforward as for the regression equations because the information regarding the importance of each input parameter is stored in a matrix of connection weights that is not easily interpretable. However, one method to examine the relative importance of various parameters is to perform an input sensitivity study. The sensitivity study is conducted by removing each input one at a time and examining its effect on the output. The correlation between predicted and actual load with a given input removed is compared to the correlation of the network with all of the inputs available and provides a measure of that variable's importance to the output. Using this method the most important input parameters in the neural network models are determined and the results are summarized in Table 8.

Summary and Conclusions

Several analytical techniques were used to examine features found in flight test data for four rotor system components. Multiple regression and neural network approaches were used to develop load prediction models that were evaluated on a broad range of different flight maneuvers. Based on the features exhibited in the data used in this study, the following conclusions can be made:

1) The low-speed/hover flight regime and the partial power/autorotative flight regime are the most difficult regimes for load prediction. Conversely, good accuracy is generally attained for level flight, moderate-g, and aggressive high-g flight.

2) Pushrod and blade normal bending models showed the highest overall accuracy with correlation coefficients ranging from 85 to 93% and normalized rms error from 5 to 8%. Damper and main rotor shaft bending loads were more difficult to predict.

3) Damper load behaves very nonlinearly across the load range. Below 3800 lb it shows very little correlation with the independent parameters used in this study and is very difficult to predict regardless of whether a regression or neural network model was used. However, for loads above 3800 lb, the damper load could be predicted with a much higher degree of accuracy.

4) Overall the neural network models performed slightly better than the regression models and resulted in approximately 10% lower rms error. Two cases where the regression equation produced higher accuracy than the neural network was for pushrod load in the high-g flight regime and for high values of damper load.

5) Dividing the data into flight regimes helps to isolate where the models perform well and where they perform poorly. Creating a separate model for each regime usually resulted in a better model for the high-g regime. For the other four regimes the overall models generally worked best.

6) An analysis of the standardized regression coefficients as well as a neural network sensitivity analysis suggests that load factor, velocity, and pilot longitudinal stick position are the most important parameters for predicting vibratory component loads in the rotor system.

Acknowledgments

The authors would like to thank Kelly McCool, DTMB, for her support in managing the flight loads database and Carl Schaefer, NAVAIRSYSCOM, for monitoring this work and for providing technical feedback and suggestions.

References

[1]Cronkhite, J. D., "Practical Applications of Health and Usage Monitoring (HUMS) to Helicopter Rotor, Engine, and Drive Systems," *Proceedings of the American Helicopter Society 49th Annual Forum* (St. Louis, MO), American Helicopter Society, Alexandria, VA, 1993, pp. 1445–1455.

[2]Spinello, M., and Maino, B., "Helicopter Usage Monitoring Systems: Aiming at Safer Operations," *Proceedings of the 19th European Rotorcraft Forum* (Cernobbio, Italy), Associazione Italiana di Aeronautica ed Astronautica and Associazione Industrie Aerospaziali, Italy, 1993, pp. E2.1–E2.10.

[3]Gustavson, B., Pellum, W., and Robeson, E., "Systematic Application of Holometric Synthesis for Cost-Effective Flight Load Monitoring," *Proceedings of the American Helicopter Society 49th Annual Forum* (St. Louis, MO), American Helicopter Society, Alexandria, VA, 1993, pp. 793–812.

[4]Gunsallus, C. T., and Robeson, E., "AH-64A Rotating Load Usage Monitoring from Fixed System Information," American Helicopter Society Structures Specialist Meeting (Williamsburg, VA), Oct. 1991.

[5]Haas, D. J., and Imber, R., "Identification of Helicopter Component Loads Using Multiple Regression," *Journal of Aircraft*, Vol. 31, No. 4, 1994, pp. 929–935.

[6]Haas, D. J., Milano, J., and Flitter, L., "Prediction of Helicopter Component Loads Using Neural Networks," *Journal of the American Helicopter Society*, Vol. 40, No. 1, 1995, pp. 72–82.